TIME EVOLUTION OF SCOUR AROUND BRIDGE ABUTMENTS

Francesco Ballio and Enrico Orsi
Politecnico di Milano, dept. I.I.A.R. (Hydraulics and Environment),
Piazza L. Da Vinci, 20133 Milano, Italy

Abstract: Local phenomena around bridge piers and abutments are generally considered to be similar; nevertheless the presence of the incoming boundary layer on the side wall in the abutment case generates extra pressure gradients and consequently a more complex vortex pattern. In the literature, experimental data for bridge abutments are relatively scarce; in particular almost no data are available for the time evolution of the scour. In this work we present the results of several long duration (3 days → 5 weeks) clear water scour laboratory tests around bridge abutments; the time evolution of the erosion process is analysed with respect to local and global characteristic values (maxima, volumes, hole shape). In particular we analyse the effect of the constriction ratio b/B between the transversal obstacle dimension and the flume width: in many practical situations abutments (or piers) obstruct a significant portion of the channel, so that the average acceleration due to constriction is expected to increase the scour effects of the local acceleration around the obstacle.

Measured values for maximum scour are poorly predicted by literature formulas. Scour depths are positively correlated with the constriction ratio, but increases are smaller than expected from literature indications. Experimental results show that models for bridge piers cannot be directly applied to abutments; in particular, time scales for the latter are significantly larger than for piers.

Key Words: bridge, abutment, scour, erosion, constriction.

1. INTRODUCTION

Many highway and railway fluvial bridges either suffered severe damage or collapsed during recent heavy floods (Morris *et al.*, 1997; Ballio *et al.*, 1998; Yeo, 1998). In spite of the considerable amount of studies on the subject in the scientific and technical literature, several hydraulic phenomena at bridge crossings are not sufficiently defined; some problems may be easily solved when designing a new bridge, by aggregating all uncertainties in safety factors, *i.e.* systematically choosing the safest model. When verifying existing bridges, the adopted approximations appear too much conservative, so that the proper assessment of bridges vulnerability (absolute or relative) is extremely difficult and questionable. Therefore, better design criteria and validation methodologies for assessment of bridge vulnerability are needed.

The large number of ongoing Research Programs promoted by National and International Companies and Agencies are a clear evidence of

the importance of the topic (Italian State Railways, National Italian Research Council (C.N.R.) and Ministry of Public Works, British Rail, Federal Highway Administration, Federal Swiss Railway). Similarly, current national and international technical/scientific regulations do not appear adequate to a safe and rational design and validation procedure of bridge waterways.

Erosion phenomena are surely one of the most important factors in bridge vulnerability: river structures are exposed to both contraction and local scour around piers and abutments. Many literature papers analyse local scour phenomena (for organised reviews and comparisons with experimental data see for example Farraday and Charlton, 1983; AA.VV., 1989; Breusers and Raudkivi, 1991; Melville, 1992; Franzetti *et al.*, 1994; Qadar and Ansari, 1994; Richardson and Davis, 1995; Melville, 1997; Kandasamy and Melville, 1998). Generalised scour due to channel constriction is less documented. Following Blench/Laursen's scheme, all models in the literature essentially adopt the same framework, i.e. the local flow constriction is conceptualised as a cross-sectional variation (among others see Laursen, 1962, 1963; Komura, 1966; Gill, 1981; Webby, 1984; AA.VV., 1989; Breusers and Raudkivi, 1991; Lim, 1993; Richardson and Davis, 1995; Umbrell *et al.*, 1998). Different experimental results often do not match well; the dependence of phenomena on some parameters whose effect is probably not of secondary importance is still not well defined; the same is true for the temporal scour evolution. Finally, abutments have been studied much less than piers with respect to erosion phenomena; prediction models for abutments are often drawn from those for piers. As a consequence, scour predictions for abutments can be affected by significant errors: studies of the Federal Highway Administration (Richardson and Devis, 1995) indicate that bridge failures for abutment scour occur at least as often as those for piers; several reports about flood damages at bridges in New Zeland are discussed in Melville (1992), showing a predominance of abutment rather than pier failures.

Local scour and contraction scour are usually studied separately (combination of pier/abutment in a "large" section channel, or "long" constriction). The contributions of these two factors are usually estimated separately and then added up without considering mutual interactions (e.g. AA.VV., 1989; Richardson and Davis, 1995); technical procedures for scour estimates at bridges only consider asymptotic values for infinite time. Preliminary evaluations have shown that this procedure might significantly overestimate the actual scour depth. As a matter of fact, generalised scour at a bridge location is often interconnected to local effects ("short" constriction).

In this paper we present the results of several long duration scour laboratory tests around bridge abutments; the erosion process was monitored by detailed measurements all around the obstacle. We will focus the analysis of results particularly on: (a) the predictability of scour with respect of its time evolution (maximum values, volumes, hole shapes) and (b) the effects of the constriction ratio *i.e.* the interactions between localised and generalised scour.

2. DIMENSIONAL ANALYSIS

The scour depth (d) at any point around a bridge abutment can be expressed in a non-dimensional form as (Crippa and Fioroni, 1999):

$$\frac{d}{\lambda} = f\left(\frac{b}{h}, \frac{b}{B}, \frac{L}{b}, \frac{\varphi}{\varphi_c}, \frac{\sigma_g}{d_{50}}, \frac{b}{d_{50}}, \text{obstacle shape}, \tau = \frac{t \cdot U}{\lambda}\right) \qquad (1)$$

Table 1. Test conditions.

Test	b	L	B	h	h_0	U	bottom slope	total test duration	b/B	b/h
	[m]	[m]	[m]	[m]	[m]	[m/s]	[%]	[hours]	[-]	[-]
A.1	0.10	0.40	1.00	0.092	0.090	0.60	0.37	863	0.10	1.09
A.2	0.10	0.40	0.60	0.095	0.094	0.65	0.37	270	0.17	1.05
A.3	0.10	0.40	0.41	0.096	0.095	0.63	0.37	281	0.24	1.04
A.4	0.10	0.40	0.30	0.099	0.103	0.69	0.37	112	0.33	1.01
A.5	0.10	0.40	0.20	0.106	0.107	0.72	0.46	270	0.50	0.94
B.1	0.10	0.40	1.00	0.183	0.183	0.70	0.17	300	0.10	0.55
B.2	0.10	0.40	0.60	0.178	0.178	0.73	0.18	80	0.17	0.56
B.3	0.10	0.40	0.40	0.177	0.177	0.72	0.21	202	0.25	0.56
B.4	0.10	0.40	0.30	0.180	0.180	0.72	0.21	143	0.33	0.56
C.1	0.05	0.20	0.50	0.093	0.093	0.64	0.38	273	0.10	0.54

where the main geometrical quantities are defined in figure 1; flow parameters (depth h, average velocity U, Shields number ϕ) refer to the position of the obstacle, for an undisturbed flow without the obstacle; d_{50} and σ_g are respectively the median size and standard deviation of the granulometric distribution; t is time; ϕ_c is the threshold value for ϕ. The characteristic length scale λ depends on the b/h ratio: typically $\lambda \propto b$ for small b/h values, while $\lambda \propto h$ for high values of the ratio (Melville, 1992 and 1997). For $1 < b/h < 25$ Melville suggests $\lambda \propto (bh)^{1/2}$. Experiments shown here have $b/h \cong 0.5 \div 1$ (see Table 1), so that either b or $(bh)^{1/2}$ may be chosen as the length scale.

Some Reynolds number should be added in the control parameter list in (1) if turbulent effects do not dominate, so that fluid viscosity affects the phenomenon. The Froude number (possibly the densimetric Froude number) could substitute for either ϕ/ϕ_c or b/d_{50} since the three non-dimensional groups are mutually correlated by h/b and the resistance equation for a developed flow.

In the following d will indicate scour depths in a generic point, d_s is the absolute scour maximum for the hole, d_{sy} the local maximum for any cross-section.

3. EXPERIMENTAL SET UP

A tilting hydraulic flume with transparent walls (length 15 m, width 1.0 m) was partially filled with a layer of sediments (density $\rho_s = 2620$ kg/m^3). The mean size diameter was $d_{50} = 5.0$ mm, with standard deviation $\sigma_g = 1.3$ mm, so that the sediment size can be considered as approximately uniform.

The bridge abutment consisted of a plexiglass prism with $b = 0.10$ m and $L = 0.40$ m (see Fig. 1), and was placed at the middle length of the flume. A smaller obstacle ($b = 0.05$ m, $L = 0.20$ m) was used in test C.1 (see Table 1). Flow depths were measured by piezometric probes at the bottom of the flume. Sediment levels were surveyed either with a depth gage or with a laser proximity sensor, which allowed detailed measurements in several transverse sections (see Fig. 1) and thus the calculation of scoured volumes around the obstacle. The

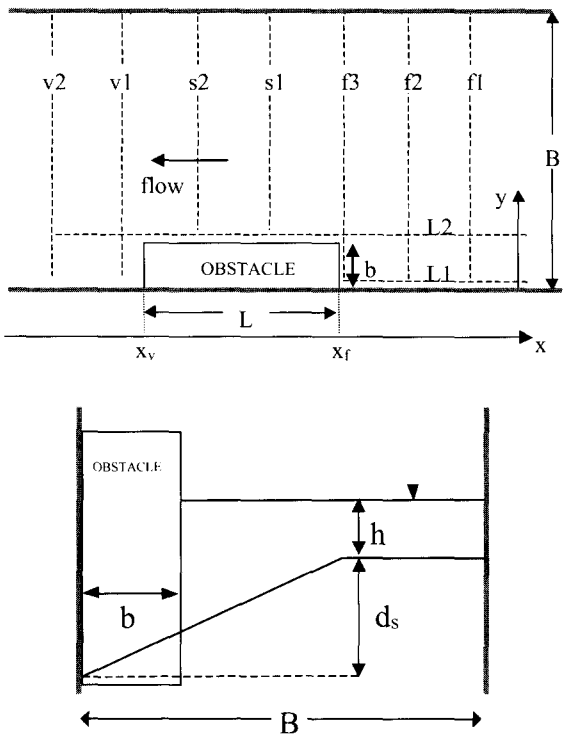

test series	x coordinates for measuring cross sections [m]						
	v2	v1	s2	s1	f3	f2	f1
A, B	8.83	9.12	9.30	9.40	9.58	9.66	9.81
C	9.01	9.15	9.24	9.29	9.38	9.42	9.50

test series	y coordinates for cross sections [m]		obstacle position [m]	
	L1	L2	x_v	x_f
A, B	2	12	9.16	9.56
C	1	6	9.17	9.37

Fig. 1. Definition Sketch

channel width was varied by coated steel plates placed along the whole channel length. The reference flow depth h was kept close to the normal depth h_o.

Experiments were run near threshold conditions. We measured sediment transport rates with small sediment traps in preliminary runs without the obstacle, identifying incipient motion conditions with some very small value of

the non-dimensional transport number Φ:

$$\Phi = \frac{q_s}{\sqrt{g\,(\rho_s/\rho - 1)\,d_{50}^3}} \cong 6 \cdot 10^{-5}$$

where q_s is the volumetric transport (pores excluded) per unit width, g is gravity and ρ is the density of water. The above value of Φ was generated by a flux of about 100 grains over a time interval of 15' and a width of 10 cm. This reference motion condition corresponds to ϕ-$\phi_c \cong 4 \cdot 10^{-4}$ when calculated with the Meyer-Peter and Müller formula, and to a visual evaluation of motion class 5 ("frequent particle movement at all locations") in Hoffmans and Verheij (1997). We chose this procedure to evaluate the threshold since we could not find a reliable estimation of the shear stress distribution between bottom and lateral walls: as the flow width B was reduced, wall effects became more and more evident, with lower sediment motion for a given value of the flow energy slope. On the basis of reasonable shear distributions we estimated $\phi_c \cong 0.040$ and $\phi/\phi_c = 0.95 \div 1.05$ for the tests discussed here, with the exception of test A.5 for which we estimated $\phi = 0.055$ for the same sediment motion conditions of the others. For details see Radice (2000).

Experimental tests have been designed so that only one non-dimensional parameter at a time in (1) was varied (see table 1); in series A and B the constriction ratio b/B is varied for given b/h values; notice that for $b/B \leq 0.09 \div 0.10$ the constriction effect on local scour is believed to be negligible (Cunha, 1973; Franzetti *et al.*, 1994). The further test (C.1) differs from the "large" tests of the two series (A.1 and B.1) either for the b or the h value, thus allowing a control for scale effects and/or for the influence of b/d_{50}.

4. EVOLUTION OF THE SCOUR PROCESS

Fig. 2 shows a typical configuration for a well developed scour hole (test B.1, end of the run): in front of the obstacle the hole has almost the form of a quarter of a cylinder, with a slope approximately equal to the sediment angle of repose in water and with the maximum close to the corner between the abutment face and the side wall; at the side of the obstacle two parallel channels can be recognised (see also cross-sections in Fig. 6): sediments coming from upstream are mainly conveyed to the bottom of the deeper channel, while the outer one is not actively affected by the sediment flux coming from the front region, and could be either linked to the erosive effect of the wake detaching from the abutment front corner, or to an alternation of active and stagnation regions within the vortex system from upstream. The erosion process typically begins at the abutment inner corner, the sediments being continuously displaced by the main flow which turns around the obstacle. After a few minutes, however, the maximum sediment activity progressively moves to the channel side, while movements are less continuous; finally the erosion process becomes mainly impulsive, and the grains are clearly forced upstream and laterally by a vortical flow with a transverse horizontal axis (front region of a horseshoe vortex). The erosive process is apparently concentrated at the bottom of the hole and of the side channel; lateral widening is caused by the consequent collapse of the hole sides. In spite of the low value of σ_g for the granulometric distribution we could notice some minor armouring at the abutment corner after the first week of run.

Typical time evolution trends for the maximum scour d_s are plotted in Fig. 3 ("large" tests:

A.1, B.1, C.1). Erosion develops at a decreasing rate, so that during the first hour the scour increased approximately as much as in the following week; after a short transient, depths increase almost linearly in a logarithmic scale for time; a lessening of the logarithmic scour rate can be recognised for test A.1 approximately after $3 \cdot 10^5$ [s], but in no case could we see any asymptotic scour value.

Transverse sections f3 for test B.1 are plotted in figure 4: y and d values are normalised by the maximum scour d_{sy} on the section (which is also the absolute maximum for the hole, d_s). It can be recognised that the hole quickly reaches a self-similar evolution; the same is true for all sections in the front region, which are comparable also among different tests. Fig. 5 plots the time evolution of λ_f/d_s, where λ_f is the cubic root of the scoured volume in the front region ($x > x_f$, see fig. 1); for the choice of time normalisation factors, see the next paragraph. It can be noticed in figures 4 and 5 that the geometry of the front region of the hole approximately scales with d_s for $\tau \geq 5 \div 8 \cdot 10^5$; moreover fig. 5 shows that the scale factors are similar for different values of the flow parameters (this observation is also confirmed by direct comparison of the sections among different tests), so that all geometrical properties of the scour hole can be drawn from the values of the maximum scour. Wider sections (and larger values for λ_f/d_s) for smaller times are consistent with the displacement of the main scour zone from the inner to the outer corner of the abutment, as previously described. Bottom profiles at the side (Fig. 6) do not show such a good self-similarity along time, nor can they be quantitatively compared among different tests, though they have qualitatively similar shapes. Moreover, Fig. 7 indicates that the scoured volume of the side region ($x_v < x < x_f$; λ_s indicates the cubic root of the corresponding volume) does not scale with d_s even for the largest time values: similarly to the front region, cross sections are wider at the beginning of the phenomenon (see also Fig. 6), but for $\tau \geq 5 \div 8 \cdot 10^5$ the λ_s/d_s ratio starts to grow, possibly also because of the reduction of sedi-

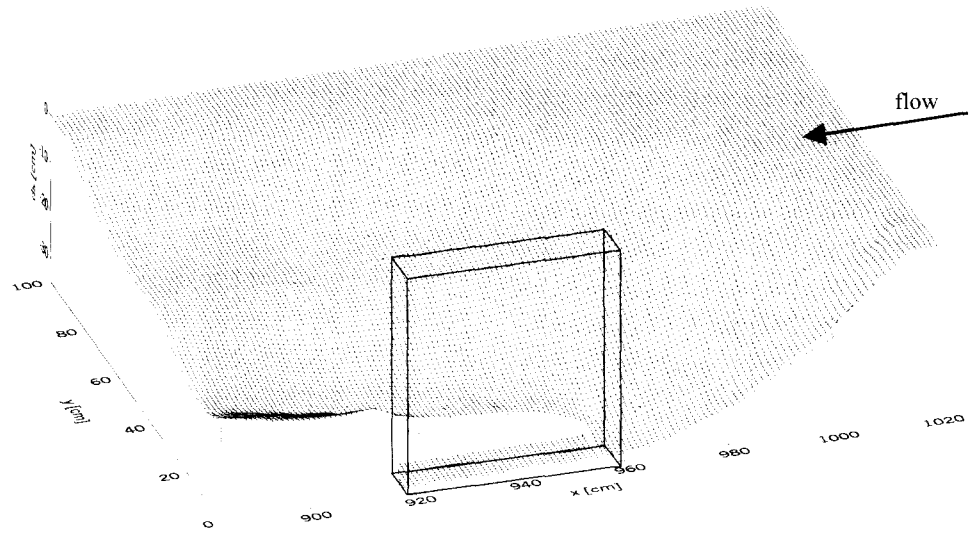

Fig. 2. Erosion Hole for Test B.1 at t = 18000 [s].

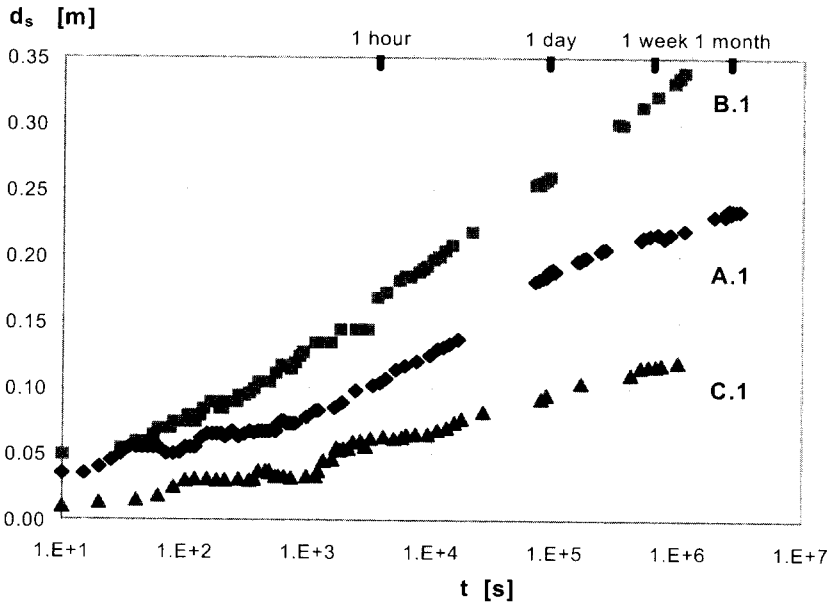

Fig. 3. Time Evolution of Maximum Scour Depth for "Large" Tests.

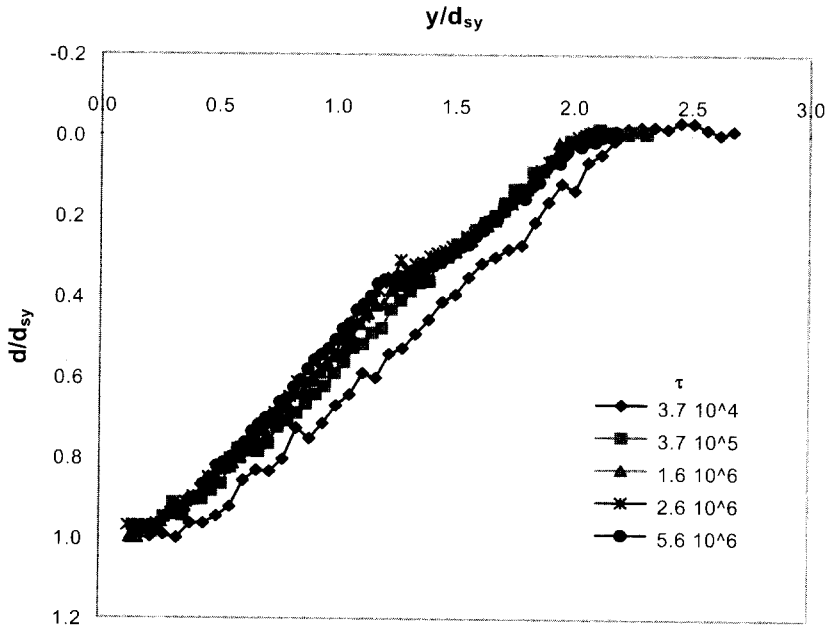

Fig. 4. Test B.1, Bottom Profiles at Section f3. $\tau = tU/(bh)^{0.5}$.

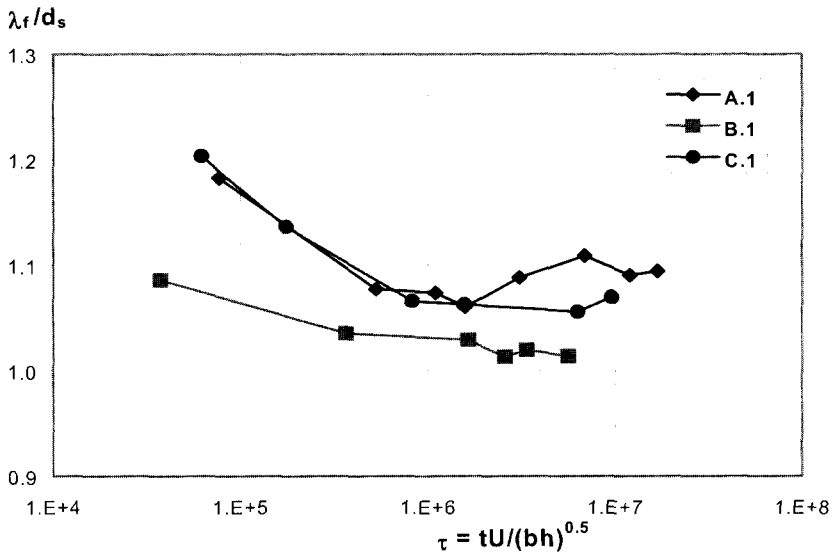

Fig. 5. "Large" Tests, Volume Scale for the Front Region ($x > x_f$).

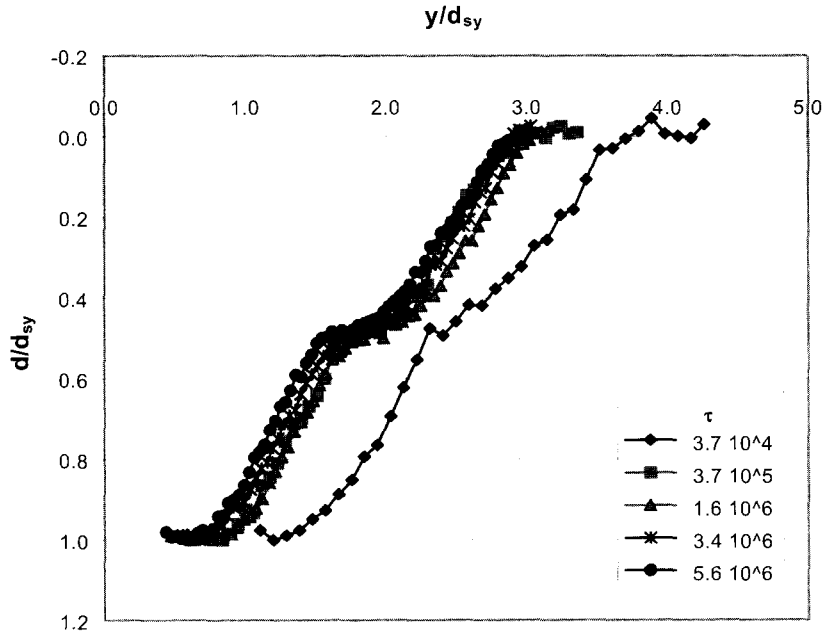

Fig. 6. Test B.1, Bottom Profiles at Section s1. $\tau = tU/(bh)^{0.5}$.

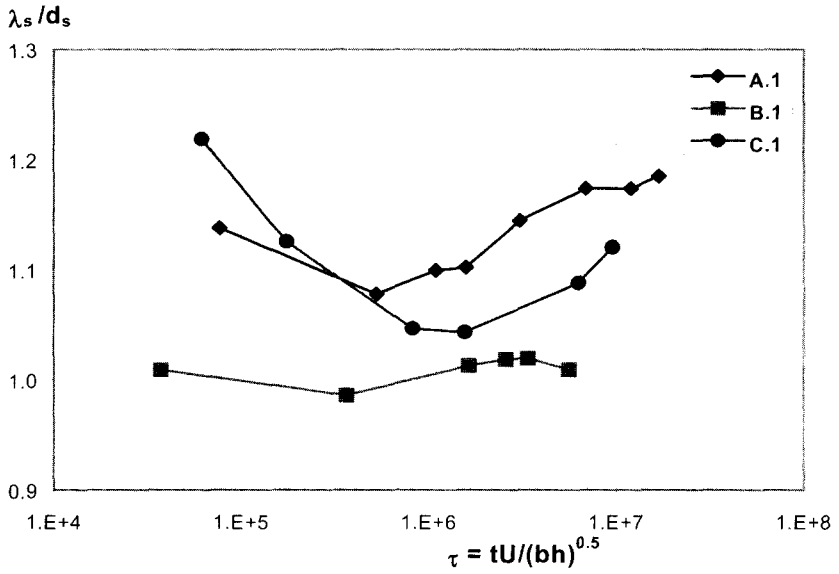

Fig. 7. "Large" Tests, Volume Scale for the Side Region ($x_v < x < x_f$).

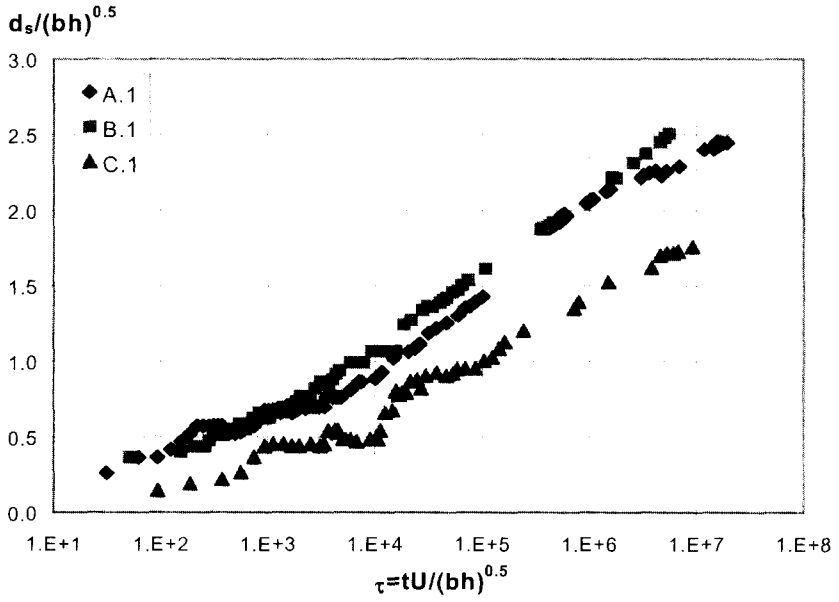

Fig. 8. Non-dimensional Time Evolution of Maximum Scour Depth for "Large" Tests. Depths Scaled with $\lambda = (bh)^{0.5}$.

ment flux from the front region. These results indicate that the interactions among the main stream, the vortex system coming from the front and the wake from the corner generate a complex flow field in the constricted reach, whose scouring effects change with time.

5. TIME EVOLUTION AND MAXIMUM SCOUR VALUES FOR NON-CONSTRICTED TESTS (B/B = 0.10)

Maximum scour values are plotted in non-dimensional form in Fig. 8. Test A.1 has $b/h \cong 1$, while test B.1 and C.1 have $b/h \cong 0.5$, so that $\lambda = b$ should be a proper scale for a comparison of the three tests according to Melville (1992); on the contrary, we found that $\lambda = (bh)^{1/2}$ works better than $\lambda = b$ with all tests, so that we will use the former scale for the normalisation of data. Tests A.1 and B.1 collapse reasonably well on a single trend, but test C.1 lies significantly underneath the other two. Tests B.1 and C.1 have similar values for all non-dimensional parameters other than b/d_{50}; literature (Melville, 1992; Franzetti *et al.*, 1994) indicates a positive correlation between the equilibrium scour values and b/d_{50} for $b/d_{50} < 30 \div 50$, which could explain why test C.1 ($b/d_{50} = 10$) has smaller values than A.1 and B.1 ($b/d_{50} = 20$). It must be noticed that the above-mentioned correlation has been drawn for low b/h values (where b dominates as length scale); we think that the dependence of the scour on the grain scale should be rather expressed in terms of λ/d_{50}, *i.e.* $(bh)^{1/2}/d_{50}$. Preliminary evaluations have supported such an assumption, which also improves the superimposition of tests A.1 and B.1. Anyway, we will apply no correction for λ/d_{50} on these results, both because we do not yet have enough data to validate our assumption and because it would have only a minor effect on the following analyses.

As already noticed, in spite of their long duration, none of our experiments reached a steady scour value. Therefore it would be useful to extrapolate the measured temporal trends to possible equilibrium values by means of analytical expressions for $d_s(t)$ from the literature. We considered several formulas (Ettema, 1980; Islam *et al.*, 1986; Franzetti *et al.*, 1994; Hoffmans and Verheij, 1997; Bertoldi and Jones, 1998; Whitehouse-in Cardoso and Bettess, 1999; Melville and Chiew, 1999) but none of them matched the measured trends. It should be noticed that most of the expressions were originally drawn for piers; Cardoso and Bettes (1999) showed that pier formulas in Franzetti *et al.*, Ettema and Whitehouse could be applied to their abutments data only after a proper modifications of the coefficients. We also tried to adapt literature expressions to our data; the formula which best matches all the tests with constant values of the coefficients turned to be that in Franzetti *et al.*:

$$\frac{d_s}{d_{se}} = 1 - e^{-\alpha\left(\frac{t \cdot U}{\lambda}\right)^{\beta}} \qquad (2)$$

where d_{se} is the equilibrium scour depth. The authors proposed this formula for cylindrical piers, with λ = pier diameter, $\alpha = 0.028$ and $\beta = 0.33$. We used $\lambda = (bh)^{1/2}$, while coefficient β had to be modified to $\beta = 0.28$. Values for d_{se} were estimated by eye-fitting measured trends to the analytical expression, with particular care for data at high times. Results are plotted in Fig. 9, which shows a reasonable agreement of the three series with expression (2).

Estimated d_{se} values are plotted together with the last measured scour value in fig. 10. The graph also shows equilibrium depths calculated with three literature formulas.

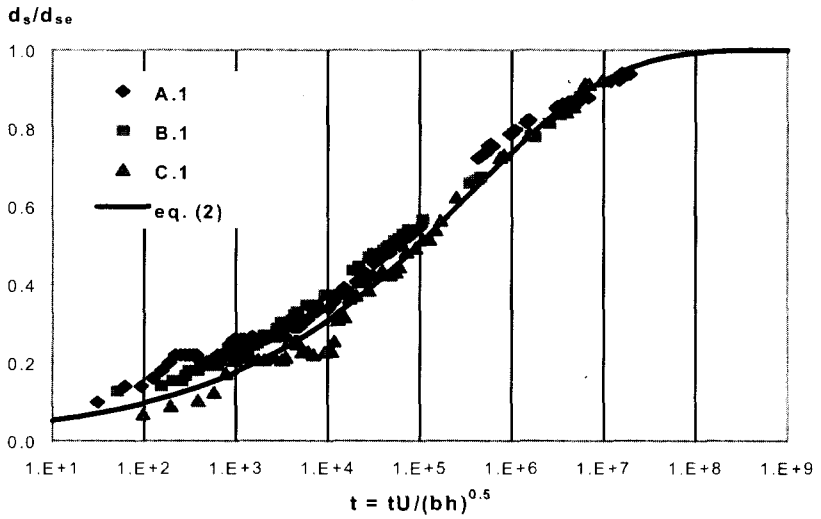

Fig. 9. Non-dimensional Time Evolution of Maximum Scour Depth for "Large" Tests. Depths Scaled with Estimated Equilibrium Values d_{se}.

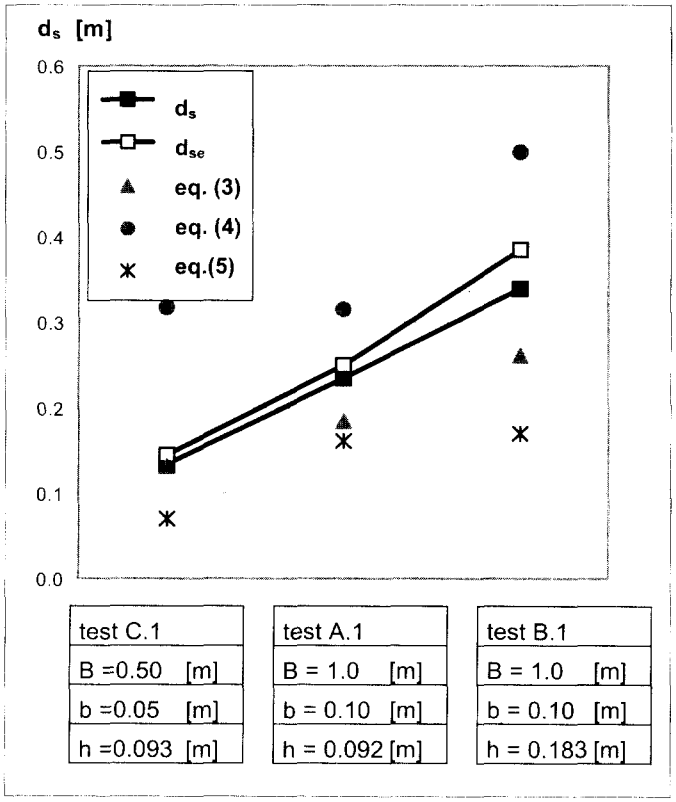

Fig. 10. "Large" Tests, Comparison of Measured and Calculated Maximum Scour Depths.

Laursen (1963) – abutment

$$\frac{b}{h} = 2.75 \cdot \frac{d_s}{h} \cdot \left[\left(\frac{1}{12} \cdot \frac{d_s}{h} + 1 \right)^{7/6} - 1 \right] \qquad (3)$$

Gill (1972) - spur dike

$$\frac{d_s + h}{h} = 8.375 \cdot \left(\frac{d_{50}}{h} \right)^{0.25} \cdot \left(\frac{B}{B-b} \right)^{6/7} \qquad (4)$$

Melville (1997) - abutment

$$\frac{d_{se}}{\lambda} = \cdot 2 \cdot K_d \; K_d = \text{function of } b/d_{50} \qquad (5)$$

Equations (3)→(5) are simplified versions of the corresponding original formulas, for the geometrical and transport conditions of our tests (rectangular obstacle, $\phi/\phi_c = 1$, uniform sediment size). In eq. (5) we used $\lambda = (bh)^{1/2}$ for test A.1 and $\lambda = b$ for tests B.1 and C.1, as suggested by the author. Coefficient K_d was evaluated from Fig. 6 in Melville (1997). Formulas are evidently unable to predict the measured scoured depths with reasonable accuracy; moreover, eqns. (4) and (5) do not simulate correctly the effects of variation of either b or h. We tested several other models for abutments, piers and spur dikes, but they did not perform better (Radice, 2000).

6. EFFECTS OF CHANNEL CONSTRICTION ($B/B = 0.10 \rightarrow 0.50$)

Figure 11 plots the dimensional time evolution of the maximum scour depth for all tests of series A and B. Both series show little dependence of d_s on the constriction ratio for $b/B \leq 0.33$, and similar qualitative temporal trends for any value of b/B. Non-dimensional scour values $d_s/(bh)^{1/2}$ are plotted versus b/B in Fig. 12 for given values of $\tau = tU/(bh)^{1/2}$. Equilibrium scour depths extrapolated with Eq. (2) are also shown. The length scale $\lambda = (bh)^{1/2}$ is a good normalisation factor for any value of the constriction ratio; corrections for λ/d_{50} would slightly improve the superimposition of the two series for each τ value, but do not change the overall appearance of the plot. It can be observed in Fig. 12 that d_s increases with b/B, but the extra scour due to the constriction remains approximately constant for any τ, so that its relative effect diminishes with time: for tests with $b/B = 0.10 \rightarrow 0.33$ we never observed an increase for the normalised maximum scour depth larger than 25% for $\tau \cong 10^4$, reducing to less than 10% for larger τ values. Only test A.5 ($b/B = 0.50$) shows significantly increased scour levels (typically 30% higher than test A.1).

Fig. 13 shows a comparison of cross sections f3 for all tests of series A at similar non- dimensional times. When normalised by the maximum scour value profiles are similar for any value of b/B, even for tests A.3, A.4 and A.5 where the scour hole is truncated by the channel side wall. It should also be noticed that in tests A.1 and A.2, where the hole did not reach the channel side opposite to the obstacle, profiles reach the original bottom level, thus indicating no general erosion at the side of the local erosion hole. Bottom profiles showed good similarity for the tests of all series; some more spread was observed at the side of the obstacle (see also Fig. 6).

We compared the measured increases in scour depths due to the constriction of Fig. 12 with literature formulas for constriction scour (see references in the introduction). The exercise showed that the simple addition of a constriction component to local erosion in order to take into account the effect of b/B, as often suggested in technical procedures, can lead to a significant overestimation of the constriction effects (up to 300%). This result is not surprising: constriction

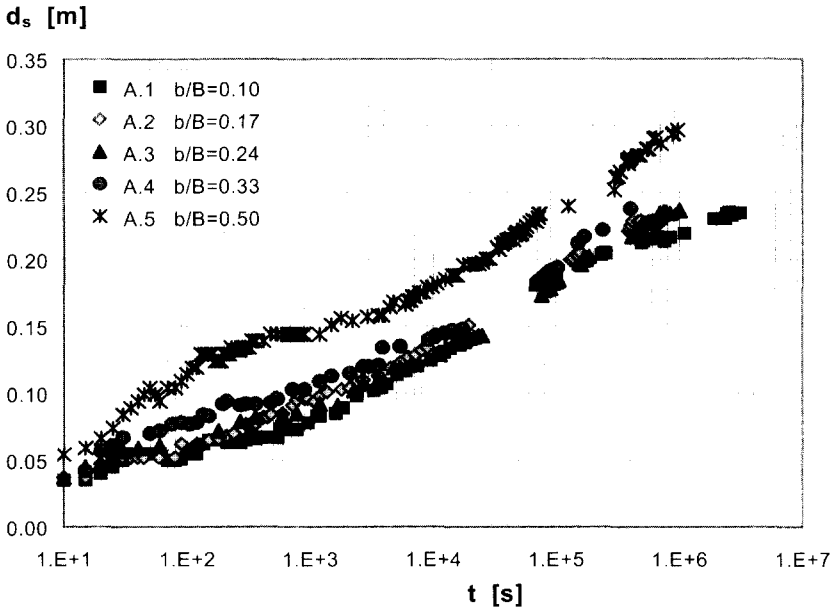

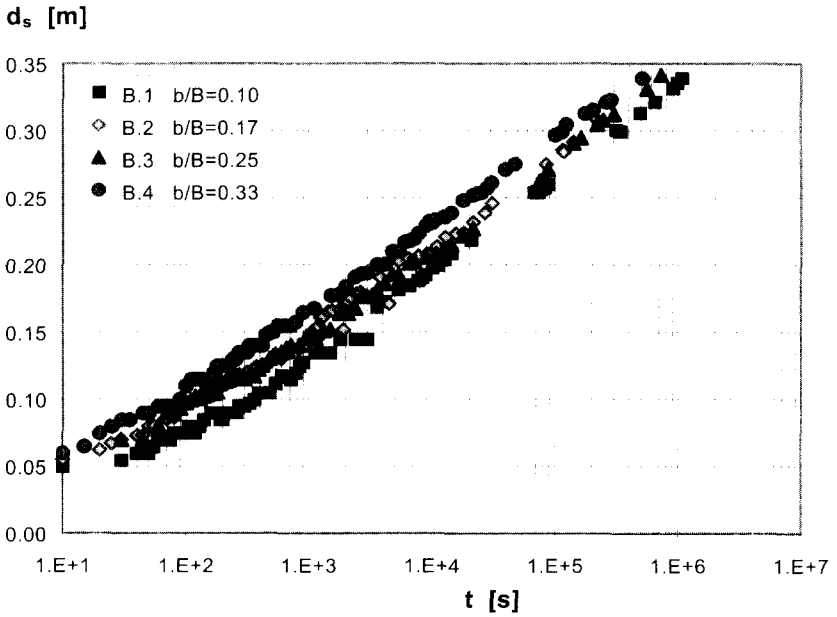

Fig. 11. Time Evolution of Maximum Scour Depth for All Tests of Series A (b/B = 0.10→0.50) and B (b/B = 0.10→0.33).

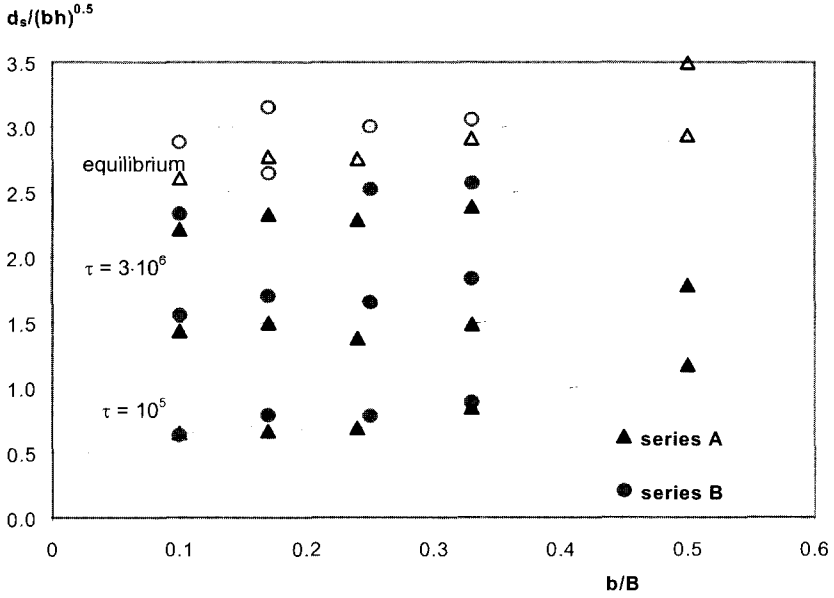

Fig. 12. Dependence of Scour Maximum Depths on b/B and Time. Empty Symbols Indicate Extrapolated Values. $\tau = tU/(bh)^{0.5}$.

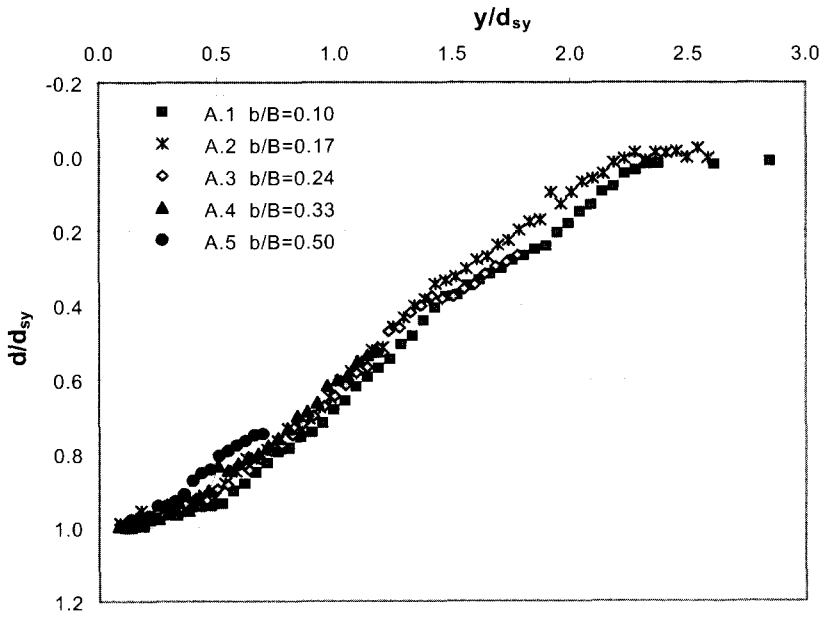

Fig. 13. Cross Sections f3 for Tests of Series A, Normalised by the Maximum Scour Depth ($2.6 \cdot 10^6 \leq \tau \leq 3.1 \cdot 10^6$).

erosion models evaluate the maximum scour depth on the base of the *average* transport condition in the constricted reach; in our experiment the transverse area of the scour hole next to the obstacle became larger than the obstructed area after a relatively short run time (typically $\tau \leq 2 \cdot 10^4$), so that the average velocity beside the obstacle was below the incipient motion condition, and no constriction erosion was expected any longer according to a model working on average values. In this sense the assumption of linear superimposition of contraction and local effects is conceptually not sound. As a matter of fact we never found evidence of any general erosion throughout the cross section, even at the very first stages of the runs, thus indicating that the flow acceleration due to the obstacle is localised close to it. In a "long" contraction the effect of the constriction gradually spreads to the whole cross section, so that a general erosion would be enhanced moving downflow, while concentrated effects extinguish; in "short" contractions, on the contrary, a significant constriction ratio increases local erosion depths more than causing general erosion.

7. CONCLUSIONS

In this work we presented the results of several long duration scour laboratory experiments around bridge abutments; experimental conditions have been chosen so that only one non-dimensional control parameter at a time was varied. Detailed measurements of the erosion holes allowed the evaluation of scoured volumes. The analysis of the results shows the following.

Temporal evolutions of scour depths for abutments are qualitatively similar to those for piers, but quantitatively different. Analytical expressions for piers can be adapted to measured values only after proper modification of the coefficients: in particular, time scales for our tests are much larger than standard values for piers.

Measured values for maximum scour depths are poorly estimated by literature formulas. Standard indications for the dominant length scale (b and/or h) are not consistent with our data.

Scour patterns show geometrical similarity along time and among different tests; even when the hole encounters the flume wall opposite to the obstacle, it is simply truncated without deformations. As a consequence, all characteristics of the scour hole which could be significant for the abutment stability (hole width, volume, ...) can be drawn with reasonable accuracy from maximum depths and/or from any other scour scale.

We observed significant effects of the constriction ratio on scour only for extreme values of the ratio ($b/B = 0.50$). If standard models are used to evaluate contraction erosion, the simple addition of contraction and local effects can lead to a significant overestimation of the total scour; a conceptual analysis of the results shows that the assumption of linear superimposition of contraction and local effects is not sound.

As a general comment, we should stress that abutment scour is less documented than pier scour, in spite of its importance on bridge vulnerability. No comprehensive synthesis of experimental data is available. As a consequence, relatively large errors should be expected when predicting abutment scour on the base of literature models.

Additional experiments are necessary to verify the present observations on a wider variety of flow conditions, especially for different b/h and h/d_{50} values. In particular, lower values for b/h should increase constriction erosion with respect to local erosion, thus enhancing the effect of b/B.

REFERENCES

AA.VV. (1989). *Hydraulic Aspects of Bridges: Assessment of the Risk of Scour*, Civil Engineering Department, Handbook n. 47, HR Wallingford.

Ballio F., Bianchi A., Franzetti S., De Falco F., Mancini M. (1998). "Vulnerabilità idraulica di ponti fluviali", *Proceedings XXVI Convegno Nazionale di Idraulica e Costruzioni Idrauliche*, Catania 9-12 September, 69-79.

Bertoldi D.A., Sterling Jones J. (1998). "Time to scour experiments as an indirect measure of stream power around bridge piers", *Proceedings of the International Water Resources Engineering Conference*, Memphis, Tennessee, 264-269.

Breusers H.N.C., Raudkivi A.J. (1991). *Scouring*, IAHR Hydraulic Structures Design Manual, A.A. Balkema edt., Rotterdam.

Cardoso A.H., Bettess R. (1999). "Effects of time and channel geometry on scour at bridge abutments", *Journal of Hydraulic Engineering*, Vol. 125, n. 4, 388-399.

Crippa, S., M. Fioroni (1999). Erosione in prossimità delle spalle dei ponti fluviali – studio sperimentale, Tesi di laurea, Politecnico di Milano.

Cunha, L.V. (1973). Discussion, Journal of Hydraulics Division, 98(HY9), pp. 1637-1639.

Ettema R. (1980). *Scour at bridge piers*, Department of civil engineering, University of Auckland, New Zealand, n. 216.

Farraday R.V., Charlton F.G. (1983). *Hydraulic factors in bridge design*, ed. Hydraulics Research Station Limited, Wallingford.

Franzetti S., Malavasi S., Piccinin C. (1994). "Sull'erosione alla base delle pile di ponte in acque chiare", *Proceedings XXIV Convegno di Idraulica e Costruzioni Idrauliche*, Napoli, Vol. II, T4 13-24.

Gill M.A. (1972). "Erosion of Sand Beds around Spur Dikes", *ASCE Journal of Hydraulic Division*, Vol. 98, n. HY9, 1587-1602.

Gill M.A. (1981). "Bed Erosion in Rectangular Long Contraction", *ASCE Journal of Hydraulic Division*, Vol. 107, n. HY3, 273-284.

Hoffmans, G.J.C.M., H.J. Verheij. (1997). *Scour Manual*, Cap. 2. A.A. Balkema, Rotterdam.

Islam M.N., Garde R.J., Ranga Raiu K.G. (1986). "Temporal variation of local scour", *Proceedings IAHR Symposium on Scale Effects in Modelling Sediment Transport Phenomena*, Toronto, 25-28 August, 252.

Kandasamy J.K., Melville B.W. (1998). "Maximum Local Scour Depth at Bridge Piers and Abutments", *Journal of Hydraulic Research*, Vol. 36, n. 2, 183-198.

Komura S. (1966). "Equilibrium Depth of Scour in Long Constrictions", *ASCE Journal of Hydraulic Division*, Vol. 92, n. HY5, 17-37.

Laursen E.M. (1962). "Scour at Bridge Crossings", *ASCE Transactions*, Vol. 127, Part I, 166-180.

Laursen E.M. (1963). "An Analysis of Relief Bridge Scour", *ASCE Journal of Hydraulic Division*, Vol. 89, n. HY3, 93-118.

Lim S.Y. (1993). "Clear Water Scour in Long Contractions", *Proceeding Institution of Civil Engineering – Water, Maritime & Energy*, Vol. 101, 93-98.

Melville B.W. (1992). "Local Scour at Bridge Abutments", *Journal of Hydraulic Engineering*, Vol. 118, n. 4, 615-631.

Melville B.W. (1997). "Pier and Abutments Scour: Integrated Approach", *Journal of Hydraulic Engineering*, Vol. 123, n. 2, 125-136.

Melville B.W., Chiew Y.M. (1999). "Time scale for local.

Morris J.L., Pagan-Ortiz J.E. (1997). "Bridge Scour Evaluation Program in the United States", *Proceedings of the 27th IAHR Congress*, S. Francisco, Theme A, 110-115.

Qadar A., Ansari S.A. (1994). "Bridge Pier-Scour Equations – An Assessment", *Proceedings of Hydraulic Engineering '94*, Buffalo NY, August 1-5, Vol. 1, 61-67.

Radice, A (2000). *Fenomeni erosivi in corrispondenza delle spalle dei ponti*, Tesi di laurea, Politecnico di Milano.

Richardson E.V., Davis S.R. (1995). *Evaluating* scour at bridge piers", *Journal of Hydraulic Research*, Vol. 125, n. 1, 59-65.

Francesco Ballio, Politecnico di Milano, dept. I.I.A.R. (Hydraulics and Environment), Piazza L. Da Vinci, 20133 Milano, Italy

(E-mail : francesco.ballio@polimi.it)

(Received October 8, 2001; accepted October 12, 2001)